after propagating 10 cm through the material is shown calculated by both the FDTD approaches outlined above. Note that the zero crossings of the two pulses occur almost exactly at the same time, indicating nearly identical propagation velocities. However, the pulse shapes are different, indicating different attenuation of the different frequency components of the pulse.

To illustrate this more clearly, both transmitted pulses in Fig. 3 were Fourier transformed to the frequency domain and divided by the Fourier transform of the incident pulse. The result is shown in Fig. 4. The constant parameter calculation produces the correct attenuation result only at 8 GHz, the frequency at which the conductivity value σ used in the calculation was determined. On the other hand, the FDTD calculation which includes the Debye pole agrees quite well with the exact solution.

References

[1] K. S. Yee, "Numerical solution of initial boundary value problems involving Maxwell's equations in isotropic media," *IEEE Trans. Antennas Propagat.*, vol. AP-14, May 1966.

[2] R. Luebbers, F. Hunsberger, K. Kunz, and R. Standler, "A frequency-dependent finite difference time domain formulation for dispersive materials," *IEEE Trans. Electromagnet. Compat.*, vol. 32, no. 3, Aug. 1990.

[3] R. Luebbers, F. Hunsberger, and K. Kunz, "A frequency-dependent time domain formulation for transient propagation in plasma," *IEEE Trans. Antennas Propagat.*, vol. 39, no. 1, Jan. 1991.

[4] R. Luebbers and F. Hunsberger, "FDTD for Nth order dispersive media," *IEEE Trans. Antennas Propagat.*, vol. 40, no. 11, pp. 1297–1301, Nov. 1992.

[5] K. Kunz and R. Luebbers, *The Finite Difference Time Domain Method for Electromagnetics*. Boca Raton: CRC Press, 1993.

[6] T. Kashiwa and I. Fukai, "A treatment of the dispersive characteristics associated with electronic polarization," *Microwave Opt. Technol. Lett.*, vol. 3, no. 6, June 1990.

[7] R. Joseph, S. Hagness, and A. Taflove, "Direct time integration of Maxwell's equations in linear dispersive media with absorption for scattering and propagation of femtosecond electromagnetic pulses," *Opt. Lett.*, vol. 16, no. 18, Sept. 15, 1991.

[8] C. A. Balanis, *Advanced Engineering Electromagnetics*. New York: John Wiley and Sons, 1989.

[9] IMSL Math Library Version 10.1, IMSL Inc., 2500 Permian Tower, 2500 City West Boulevard, Houston, TX, 77042-3020.

Computer-Aided Design of Multilayered Dielectric Frequency-Selective Surfaces for Circularly Polarized Millimeter-Wave Applications

Jens Bornemann, *Senior Member, IEEE*

***Abstract*—A procedure for the computer-aided design of dielectric-layered frequency-selective surfaces is introduced. Emphasis is placed on millimeter-wave applications involving circularly polarized incident signals. The design routine incorporates filter theory for high–low impedance structures and analysis concepts known from thin-film optics which include the losses of the materials. For given material constants and performance specifications, the exact thicknesses of the dielectric layers as well as the angle of the incident wave are determined by applying optimization strategies. A 40-GHz design example demonstrates the attractiveness of the design in circularly polarized millimeter-wave frequency-selective surface applications.**

Manuscript received December 23, 1992; revised June 1, 1993.

The author is with the Centre for Advanced Materials and Related Technology (CAMTEC), Department of Electrical and Computer Engineering, University of Victoria, Victoria, B.C., Canada V8W 3P6.

IEEE Log Number 9213067.

I. Introduction

Frequency-selective surfaces (FSS's) for microwave systems are commonly fabricated in printed-circuit technology where the selectivity is determined by the shape and spacing of elements within an array of conducting patches. Theoretical and experimental investigations have focused on dipoles [1], both loaded [2] and crossed dipoles [3], [4], tripoles [5], square loops [6], [7], rings [8], [9], and, recently, on more complex structures, e.g., [10], [11]. While these configurations work well in the microwave range, the application of such metallic screens at millimeter-wave frequencies becomes questionable owing to increasing absorption losses and the influence of the finite metallization thickness.

A millimeter-wave surface composed of alternating dielectric bars has been proposed in [12]. Although the structure provides a reasonable transmission bandwidth for TE-wave operation, the reflection bandwidth is extremely narrow (below 2.5%), thus severely limiting its application. These drawbacks can be eliminated by using stratified dielectric layers [13]. Not only is the bandwidth significantly increased, but also similar (magnitude) responses can be obtained if either a TE or TM wave incident. However, phase responses obtained for TE and TM waves are generally not identical as required in circularly polarized applications. Therefore, horizontally or vertically layered dielectric surfaces—as well as printed-circuit structures theoretically investigated up to 80 GHz, e.g., [4]—cannot immediately be used in millimeter-wave applications involving circular polarization.

This paper focuses on the computer-aided design of multilayered dielectric FSS's for circularly polarized millimeter-wave applications. The design procedure is based on the high–low impedance concept which is well known from guided-wave low-pass filter applications, e.g., [14], where the incident wave is perpendicular to the layered structure, and from thin-film optical filters, e.g., [15], where oblique incidence is utilized. The formulation related to the latter application is used in this paper to obtain TE- and TM-wave responses of multilayered dielectric surfaces. For an arbitrary angle of incidence and under the consideration of material losses, both magnitude and phase characteristics of the frequency-selective surface are analyzed. While initial dimensions are obtained from standard low-pass filter design [14], [16], an optimization procedure determines the final dimensions of the FSS for suitable operation with circularly polarized waves. With the rapid progress in material technology, especially the ability of growing multilayered substrates, the design is also suitable for other applications such as radomes and anti- or high-reflective coatings.

II. Theory

The analysis of a given multilayered structure (Fig. 1) of complex relative permittivities $\epsilon_{ci} = \epsilon_{ri}(1 - j \tan \delta_i)$ is well known from thin-film optics, particularly thin-film optical filters [15], and can be performed by separately solving the one-dimensional problems related to TE- and TM-wave excitation. With the electric field at $z = D$ (cf. Fig. 1) normalized to unity and the corresponding magnetic field represented by the normalized admittance p_0 at $z = D$, the multilayered structure of individual

0018-926X/93$03.00

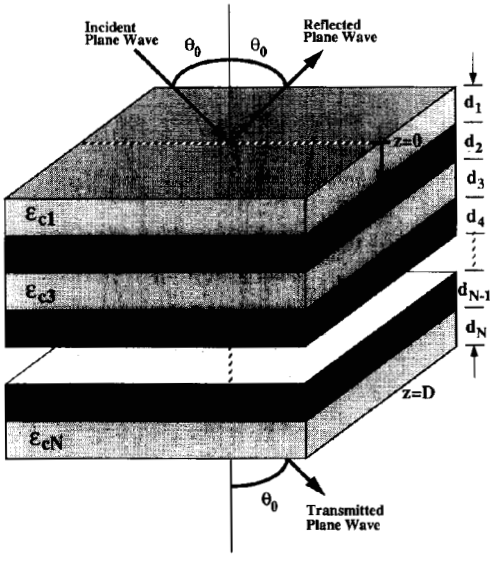

Fig. 1. Frequency-selective surface for circularly polarized millimeter waves.

layers $i = 1$ to N can be represented by [15]

$$\begin{bmatrix} B \\ C \end{bmatrix} = \prod_{i=1}^{N} \begin{bmatrix} \cosh(\gamma_i d_i) & (1/p_i)\sinh(\gamma_i d_i) \\ p_i \sinh(\gamma_i d_i) & \cosh(\gamma_i d_i) \end{bmatrix} \begin{bmatrix} 1 \\ p_0 \end{bmatrix}, \quad (1)$$

where

$$\gamma_i = \alpha_i + j\beta_i = jk_0\sqrt{\epsilon_{ci}}\cos\vartheta_i, \quad (2)$$

$$p_i = \begin{cases} \cos\vartheta_i, & \text{for TE waves,} \\ \dfrac{1}{\cos\vartheta_i}, & \text{for TM waves} \end{cases} \qquad i = 0, 1, \ldots, N, \quad (3)$$

k_0 is the free-space wave number, and d_i and ϑ_i are the thickness and refractive angle, respectively, of the ith layer. In principle, the expression in (1) represents the product of the individual transmission line matrices. The normalization is used to formulate the problem in terms of material parameters and to create a reference for, in this case, the transmitted wave at $z = D$. Consequently, B and C in (1) correspond to a normalized quantity related to the electric field component and a normalized admittance related to the magnetic field component, respectively, at $z = 0$ (Fig. 1). For details, the reader is referred to [15].

The reflection and transmission coefficients can now be written in terms of p_0, B, C,

$$r = \frac{p_0 - C/B}{p_0 + C/B}, \quad (4)$$

$$t = \frac{2p_0}{p_0 B + C}, \quad (5)$$

which define reflectance R, transmittance T and absorption A:

$$R = rr^*, \quad (6)$$

$$T = tt^* = \frac{p_0(1-R)}{\mathrm{Re}\{BC^*\}}, \quad (7)$$

$$A = 1 - R - T = (1-R)\left[1 - \frac{p_0}{\mathrm{Re}\{BC^*\}}\right]. \quad (8)$$

(The asterisk denotes the complex conjugate.) For elliptically polarized waves (TE + TM), the ellipticity is calculated from

$$\frac{\text{ellipticity}}{\text{dB}} = 20\log\frac{E_{\max}}{E_{\min}}, \quad (9)$$

where the minima and maxima of the electric field, i.e., the two axes of the ellipse, occur at angles

$$\Psi = \frac{S_{\mathrm{TE}}\sin(2\phi_{\mathrm{TE}}) - S_{\mathrm{TM}}\sin(2\phi_{\mathrm{TM}})}{-S_{\mathrm{TE}}\cos(2\phi_{\mathrm{TE}}) + S_{\mathrm{TM}}\cos(2\phi_{\mathrm{TM}})} \mp n\frac{\pi}{2}. \quad (10)$$

For the reflected and transmitted wave, $S_{\mathrm{TE,TM}}$ is given by R and T from (6) and (7), respectively, and the related phases $\phi_{\mathrm{TE,TM}}$ are obtained from (4) and (5). Note that if TE and TM responses are identical, (10) becomes useless since $E_{\max} = E_{\min}$, and the resulting wave is circularly polarized.

The design of the FSS is carried out by using standard low-pass filter theory for the transmission band and the high-low impedance concept, e.g., [16], to calculate the initial thicknesses of the layers

$$d_i = \frac{g_i}{k_0\sqrt{\epsilon_{ri}}} \begin{cases} \dfrac{p_0}{p_i} & \text{for a high-permittivity dielectric,} \\ \dfrac{p_i}{p_0} & \text{for a low-permittivity dielectric,} \end{cases} \quad (11)$$

where g_i are the low-pass filter coefficients. For given material constants ϵ_{ri}, two sets of layer thicknesses d_i—one for TE-wave and one for TM-wave excitation—are obtained from (11). Therefore, initial values are taken as the average of the two sets. A final optimization varies the thicknesses d_i of the layers and the incident angle θ_0 (cf. Fig. 1) until given specifications are met. It is obvious from (3) that any optimization procedure would tend to lower the incident angle to zero to obtain identical magnitude and phase responses for TE- and TM-wave excitation. Since this is not practical for the application as a FSS, a minimum angle must be specified.

It should be noted that with the rapid progress in material technology, especially the ability of growing multilayered substrates of, to a certain degree, selectable material characteristics, also the values ϵ_{ri} might be chosen as optimization parameters. It is expected that this possibility leads to the degree of freedom required in the optimization process either to operate the structure at different incident angles or to enhance the stability of responses by using periodic blocks of multilayered materials.

III. Results

Without loss of generality, dielectric materials RT/Duroid 6010.5 ($\epsilon_H = 10.5[1 - j0.0023]$) and RT/Duroid 5880 ($\epsilon_L = 2.20[1 - j0.0009]$) have chosen [17] as design examples. Since high-low impedance structures require the connected-line impedance to lie between the highest and lowest impedance values, a fictive medium of $\epsilon_N = \epsilon_{rL}^2 = 4.84$ is used for normalization purposes in this case of only two different materials. However, the so-obtained design uses a high-dielectric material as the top and bottom layer. This creates interfaces of relatively high reflection coefficients and, therefore, a quarter-wavelength transformer section of low-dielectric layer (ϵ_L) is used to achieve a reasonable match to free space.

Fig. 2(a) shows the responses of a seven-layer FSS designed by the procedure outlined in [13]. Based on a bandwidth definition

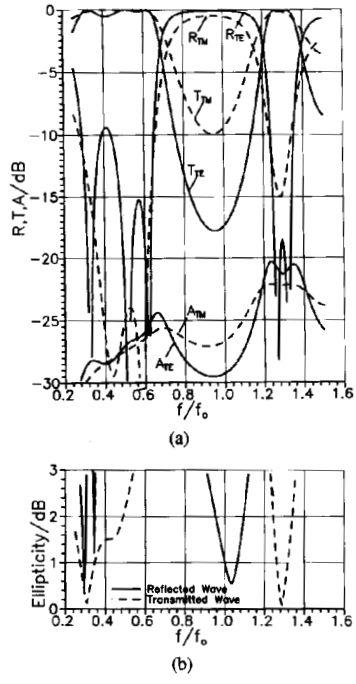

Fig. 2. Frequency response of a seven-layer FSS with $\theta_0 = 45°$ optimized using the method of [13]; $\epsilon_{c(2n+1)} = \epsilon_H$, $\epsilon_{c2n} = \epsilon_L$ $(n = 0, \ldots, 3)$. (a) Reflectance R, transmittance T, and absorption A (subscripts denote mode of excitation); (b) ellipticity.

of 90% transmitted or reflected power, wide frequency ranges for the transmitted ($f/f_0 = 0.26$ to 0.66) and reflected ($f/f_0 = 0.8$ to 1.08) signals are obtained for both TE and TM-wave excitation. However, this design has two disadvantages. First, less than 10-dB isolation is obtained for the TM excitation in the reflection band (at $f/f_0 = 0.94$) and for the TE excitation in the transmission band (at $f/f_0 = 0.41$). This is owing to the fact that this design incorporates high-dielectric material as the outermost layers which, as mentioned above, results in a high amount of reflection. Second, the ellipticities of reflected and transmitted waves show an extremely narrowband behavior [Fig. 2(b)]. Therefore, this design would leave an incident circularly polarized wave with an unacceptably high amount of ellipticity for both reflected and transmitted waves.

The response of a FSS designed with the procedure outlined in this paper is shown in Figs. 3 and 4. The structure is based on a seven-layer surface with two additional layers for matching purposes. Specifications have been set to provide a 10% ($0.1f_0$) bandwidth at $f/f_0 = 0.47$ (transmission) and 0.96 (reflection), 20-dB isolation, and a maximum of 1-dB ellipticity. The minimum incident angle has been set to 25° in the optimization process. Fig. 3(a) displays the reflectance, transmittance, and absorption responses which meet all of the above criteria. Due to the low-loss tangents of the materials chosen, the absorption is only around -25 dB in both bands. The optimized thicknesses for an application at $f_0 = 40$ and 4 GHz bandwidths are given in the legend of Fig. 3.

Fig. 3(b) and 3(c) show the related responses if the incident angle is varied by $+5°$ [Fig. 3(b)] and $-5°$ [Fig. 3(c)]. As is obvious from a comparison of Fig. 3(b) and (c) with Fig. 3(a), the effect of the variation of the incident angle is only marginal. As

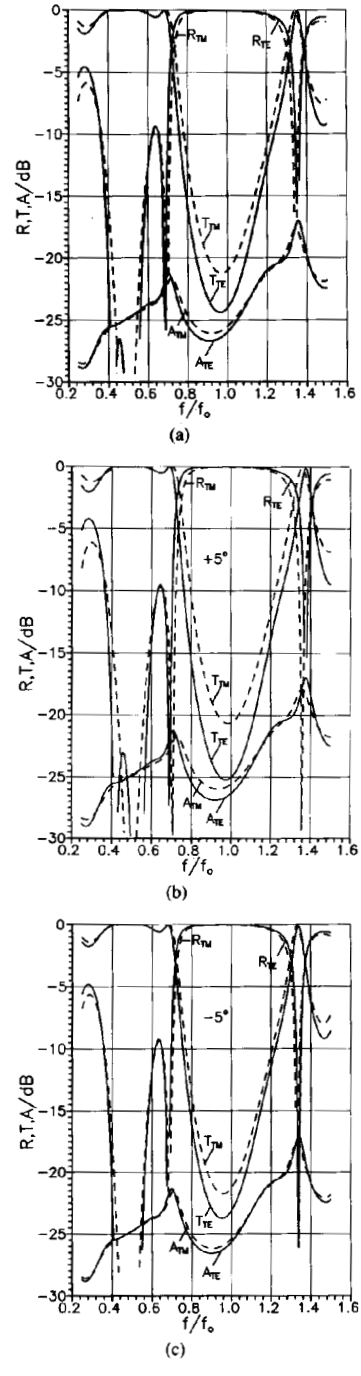

Fig. 3. Magnitude response of a seven-plus-two-layer FSS designed with this method; $\epsilon_{c(2n+1)} = \epsilon_L$, $\epsilon_{c2n} = \epsilon_H$ $(n = 0, \ldots, 4)$. Dimensions for $f_0 = 40$ GHz: $d_1 = d_9 = 3.139$ mm, $d_2 = d_8 = 0.55$ mm, $d_3 = d_7 = 1.269$ mm, $d_4 = d_6 = 0.497$ mm, $d_5 = 1.666$ mm. (a) Reflectance R, transmittance T, and absorption A for an incident angle of $\theta_0 = 25°$; (b) performance for incident-angle variation of $+5°$; (c) performance for incident-angle variation of $-5°$.

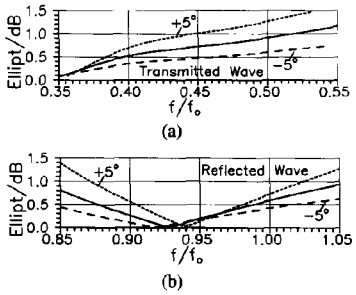

Fig. 4. Phase response of FSS specified in Fig. 3. Solid lines, $\theta_0 = 25°$; dotted lines, variation of incident angle by $+5°$; dashed lines, variation of incident angle by $-5°$. (a) Ellipticity of transmitted wave; (b) ellipticity of reflected wave.

expected from the discussion following (11), a lower incident angle improves the performance slightly [Fig. 3(c)] since it comes closer to the theoretically ideal—but not practical—value of 0°. Therefore, the performance at $-5°$ variation remains entirely within specifications. For a variation of up to $+5°$, however, some slight frequency and amplitude shifts occur, especially for TM excitation (dashed lines), which affect the performance of the FSS at the lower band edges. The isolation drops from 20 to 17.2 and 19.2 dB at the lower band edges of the transmission and reflection band, respectively. All other parameters related to magnitude responses remain within specifications.

The solid lines in Fig. 4 demonstrate that the ellipticity specifications also are met for the transmitted [Fig. 4(a)] and reflected [Fig. 4(b)] signal. Again, we find that a reduction in incident angle leads to an improved performance (dashed lines). An angle of 5° higher than specified results in increased ellipticities of both transmitted and reflected waves (dotted lines). With respect to the specified bandwidth of $0.1f_0$, however, only the transmitted signal exceeds the specified ellipticity (1 dB) by 0.39 dB while the ellipticity of the reflected wave remains below 1 dB.

IV. Conclusion

A design procedure for multiple dielectric-layered frequency-selective surfaces in circularly polarized millimeter-wave applications is presented. Standard filter theory for high–low impedance structures is used to determine the initial values of a configuration. Optical principles are applied for the analysis, and a final optimization procedure varies the incident angle and layer thicknesses until a specified behavior is obtained. Since the ellipticities of reflected and transmitted waves are considered in the optimization routine, the surface can be optimized especially for incident waves of circular polarization. An example for 40-GHz operation with 4-GHz transmission and reflection bandwidth demonstrates that this design offers an attractive solution for circularly polarized millimeter-wave FSS applications.

Acknowledgment

The author would like to thank Lizhong Sun of McGill University in Montreal, Canada, for helpful suggestions and discussions.

References

[1] R. H. Ott, R. G. Kouyoumjian, and L. Peters, "Scattering by a two-dimensional periodic array of narrow plates," *Radio Science*, vol. 2, pp. 1347–1349, Nov. 1967.

[2] B. A. Munk, R. G. Kouyoumjian, and L. Peters, "Reflection properties of periodic surfaces of loaded dipoles," *IEEE Trans. Antennas Propagat.*, vol. AP-19, pp. 612–617, Sept. 1971.

[3] S. M. A. Hamdy and E. A. Parker, "Influence of lattice geometry on transmission of electromagnetic waves through arrays of crossed dipoles," *IEE Proc. H*, vol. 129, pp. 7–10, Feb. 1982.

[4] C. Tsao and R. Mittra, "Spectral-domain analysis of frequency selective surfaces comprised of periodic arrays of cross dipoles and Jerusalem crosses," *IEEE Trans. Antennas Propagat.*, vol. AP-32, pp. 478–487, May 1984.

[5] J. C. Vardaxoglou and E. A. Parker, "Performance of two tripole arrays as frequency-selective surfaces," *Electron. Lett.*, vol. 19, pp. 709–710, Sept. 1983.

[6] R. J. Langley and E. A. Parker, "Equivalent circuit model for arrays of square loops," *Electron. Lett.*, vol. 18, pp. 294–296, Apr. 1982.

[7] ____, "Double-square frequency-selective surfaces and their equivalent circuit," *Electron. Lett.*, vol. 19, pp. 675–677, Aug. 1983.

[8] R. Cahill and E. A. Parker, "Crosspolar levels of ring arrays in reflection at 45° incidence: Influence of lattice spacing," *Electron. Lett.*, vol. 18, pp. 1060–1061, Nov. 1982.

[9] ____, "Concentric ring and Jerusalem cross arrays as frequency-selective surfaces for a 45° incidence diplexer," *Electron. Lett.*, vol. 18, pp. 313–314, Apr. 1982.

[10] E. A. Parker and A. N. A. El Sheikh, "Convoluted array elements and reduced size unit cells for frequency-selective surfaces," *IEE Proc. H*, vol. 138, pp. 19–21, Feb. 1991.

[11] A. Caroglanian and K. J. Webb, "Study of curved and planar frequency-selective surfaces with nonplanar illumination," *IEEE Trans. Antennas Propagat.*, vol. 39, pp. 211–217, Feb. 1991.

[12] H. L. Bertoni, L. S. Cheo, and T. Tamir, "Frequency-selective reflection and transmission by a periodic dielectric layer," *IEEE Trans. Antennas Propagat.*, vol. 37, pp. 78–83, Jan. 1989.

[13] L. Sun and J. Bornemann, "Frequency-selective surfaces formed by stratified dielectric layers," in *1992 IEEE-APS Intl. Symp. Dig.*, 1992, pp. 408–411.

[14] G. Matthaei, L. Young, and E. M. T. Jones, *Microwave Filters, Impedance-Matching Networks, and Coupling Structures*. Dedham, MA: Artech House, 1980.

[15] H. A. Macleod, *Thin-Film Optical Filters*. London: Adam Hilger Ltd., 1969.

[16] D. M. Pozar, *Microwave Engineering*. Reading, MA: Addison-Wesley, 1990.

[17] RT/Duroid, Rogers Corporation, TR2692, July 1981.

Improvement in Front-to-Back Ratio of a Bifilar Backfire Helix by a Flared Open End

Hisamatsu Nakano, *Fellow, IEEE,* Shin'ichi Iio, and Junji Yamauchi, *Member, IEEE*

***Abstract*—The current distribution of a bifilar helical antenna which radiates a circularly polarized wave in the backward endfire direction is decomposed into forward and reflected currents, and the contribution of each current to the radiation is evaluated numerically. Calculations show that the presence of the reflected current deteriorates the front-to-back (F/B) ratio of radiation. To reduce the reflected current and to improve the F/B ratio, flaring of the open end is proposed and investigated. The flared configuration leads to an improved F/B ratio, with an almost constant input impedance.**

I. Introduction

Patton [1] described the basic concepts of backfire radiation from a bifilar helical antenna as part of an investigation of the

Manuscript received February 5, 1993; revised July 2, 1993.

The authors are with the College of Engineering, Hosei University, 3-7-2, Kajino-cho, Koganei, Tokyo 184, Japan.

IEEE Log Number 9213066.